

Immunolocalization and functional analysis of *Opisthorchis viverrini*-M60-like-1 metallopeptidase in animal models

Research Article

Cite this article: Wendo WD, Tangkawattana S, Saichua P, Ta BTT, Candra ARK, Tangkawattana P, Suttiprapa S (2022). Immunolocalization and functional analysis of *Opisthorchis viverrini*-M60-like-1 metallopeptidase in animal models. *Parasitology* **149**, 1356–1363. <https://doi.org/10.1017/S0031182022000403>


Received: 5 February 2022
Revised: 22 March 2022
Accepted: 22 March 2022
First published online: 21 April 2022

Key words:

Immunolocalization; metallopeptidase; mucin; mucinase; *Opisthorchis viverrini*; *Ov*-M60-like-1

Authors for correspondence:

Sirikachorn Tangkawattana, E-mail: sirikach@kku.ac.th; Sutas Suttiprapa, E-mail: sutasu@kku.ac.th

Woro D. Wendo^{1,2,3}, Sirikachorn Tangkawattana^{1,4}, Prasert Saichua^{4,5},
Binh T. T. Ta⁵, Agatha R. K. Candra⁶, Prasarn Tangkawattana¹
and Sutas Suttiprapa^{4,5} 

¹Faculty of Veterinary Medicine, Khon Kaen University, Khon Kaen 40002, Thailand; ²Graduate School, Khon Kaen University, Khon Kaen 40002, Thailand; ³Department of Anatomy, Faculty of Veterinary Medicine, Universitas Gadjah Mada, Yogyakarta, Indonesia; ⁴Tropical Disease Research Center, WHO Collaborating Centre for Research and Control of Opisthorchiasis, Khon Kaen University, Khon Kaen 40002, Thailand; ⁵Tropical Medicine Graduate Program, Academic Affairs, Faculty of Medicine, Khon Kaen University, Khon Kaen 40002, Thailand and ⁶Department of Biomedicine, School of Life Sciences, Indonesia International Institute for Life Sciences, Jakarta, Indonesia

Abstract

Host mucins have crucial physical roles in preventing the parasitic establishment and maturation, and also in expelling the invading parasites. However, some parasites utilize mucinase enzymes to facilitate the infection. Recently, we have identified a mucinase enzyme of the liver fluke *Opisthorchis viverrini*, *Ov*-M60-like-1, which exhibits metallopeptidase activity against bovine submaxillary mucin substrate. Here, we aimed to study the localization of this enzyme in *O. viverrini* and the bile duct of hamsters using immunohistochemistry and functional analysis by mucin digestion in hamsters and mice tissues. The results showed that *Ov*-M60-like-1 was detected strongly in the tegument, tegumental cells, vitelline glands and mature eggs with miracidium. Expression in the gut, ovary and testis of the parasite was moderate while parenchyma showed slight colour intensity. In addition, the mucinase was also detected in the host biliary epithelial cells and goblet cells surrounding the worm. The mucinase assay revealed that the *Ov*-M60-like-1 could digest neutral mucin in the parenchyma, testis and seminal receptacle, but not the mucin in the tegument, tegumental cells and vitelline glands of the worm. The enzyme can also digest mucin in the cholangiocytes and modified the mixture type in the bile duct goblet cells of the infected hamsters, a susceptible host. In contrast, the enzyme was unable to digest neutral, acid and mixture mucin in the bile duct of the mice, a non-susceptible host. These findings indicate that *Ov*-M60-like-1 may have functions in both housekeeping tasks and host–parasite interactions, especially in modification of host susceptibility.

Introduction

Mucins play important roles in host–parasite interactions. Mucin is the main component in mucus which is a crucial defensive barrier of the host to parasite infection. Host mucins have roles in preventing parasite establishment and/or in parasite expulsion (Hasnain *et al.*, 2013). Mucin glycoproteins are secreted in large quantities by mucosal epithelia to protect the epithelial cells from toxic substances and invading microorganisms (Linden *et al.*, 2008). Although mammalian hosts have mucosal immunity to protect themselves from mechanical/chemical injuries caused by parasites, parasites have specific enzymes and mechanisms to invade the barrier and utilize host mucin as a nutrient source (Theodoropoulos *et al.*, 2001). A carcinogenic liver fluke, *Opisthorchis viverrini* (*Ov*), is the parasite that induces bile duct cancer or cholangiocarcinoma. The host–parasite interactions, including susceptibility to infection, are needed to be clarified particularly the *O. viverrini* establishment in the host's biliary tract. The studies on *O. viverrini* excretory–secretory (OVES) products suggested that various protease enzymes such as cysteine protease, cathepsin B1, asparaginyl endopeptidase and aspartic proteases are important for fluke development, nutrient acquisition, homeostasis and survival (Suttiprapa *et al.*, 2018). However, the information of enzymes being employed by the parasites for their survival in the mucin-rich environment in the bile duct of the host is still limited and unclear.

M60-like-1 metallopeptidase or *Ov*-M60-like-1 mucinase has recently been reported as the most abundant protein in the OVES (Ta *et al.*, 2020). The active monomeric enzyme contains 885 amino acids with a molecular weight of 100.43 kDa. Such *N*-glycosylated enzyme is believed to degrade mucin/mucus that protects host biliary epithelium. It was proposed as the key enzyme to degrade the mucin barrier of the bile duct. The activity of the mucinase could play a crucial role in helminth establishment and survival in the host. An *in vitro* study demonstrated that M60-like-1 metallopeptidase in the OVES could effectively digest bovine sub-maxillary mucin (Ta *et al.*, 2020). However, localization and direct effect of

Ov-M60-like-1 mucinase against the host biliary epithelial mucin/mucus have not been determined. The study was designed to demonstrate the distribution of *Ov*-M60-like-1 in the mature adult *O. viverrini* worms and also in the biliary epithelial cells of hamsters as the susceptible host and mice as the non-susceptible host of *O. viverrini* infection. The investigation employs immunohistochemistry and the functional activity of the enzyme to elucidate its role in worm biology, host–parasite interaction and host susceptibility.

Materials and methods

Animal tissues

Liver tissues of *O. viverrini*-infected Syrian golden hamsters and BALB/c mice in paraffin blocks were obtained from the project titled ‘Comparative Immunopathology of Liver Fluke Infection in Susceptible and Non-susceptible Animal Models’. The research was approved by the KKKU Animal Ethics Committee (AEKKU 78/61, IACUC KKKU 57/2563). Both animals were fed with 50 *O. viverrini* metacercariae by intragastric intubation according to the standard protocol (Lvova *et al.*, 2012) and anaesthetized with isoflurane and sacrificed on days 1, 2, 7, 14, 28 and 56 post-infection (p.i.). The liver organs were dissected into 0.5 cm thickness and fixed with 10% neutral buffered formalin overnight at room temperature. Liver tissues of the infected hamsters at day 56 p.i. and mice at days 14 and 28 p.i. were selected because maximum mucin production in hamsters and mice was observed in those designated days. Three liver sections from each of 3 *O. viverrini*-infected hamsters (day 56 p.i.) and mice (days 14 and 28 p.i.) were examined using mucinase assay. The tissue blocks were cut into 4 μ m thickness and stained with haematoxylin and eosin for histologic screening. The unstained slides were processed through immunohistochemistry for *Ov*-M60-like-1 localization and functional mucinase assay. The paraffin was removed completely in the series of xylene and rehydrated in the serial ethanol solutions and tap water prior treated with recombinant *Ov*-M60-like-1 mucinase.

Recombinant *Ov*-M60-like-1

Purified recombinant *Ov*-M60-like-1 was produced as previously described (Ta *et al.*, 2020). Briefly, the recombinant pET15b plasmid containing the coding region of *Ov*-M60-like-1 was transformed to the BL21 (DE3) strain of *Escherichia coli*. The recombinant protein expression was induced by 1 mM isopropyl β -D-1-thiogalactopyranoside. The inactive proteins in the inclusion body were denatured and refolded to collect the active form by using the SDS-KCl refolding protocol with a slight adjustment (He and Ohnishi, 2017). The refolded r*Ov*-M60-like-1 protein was purified by size-exclusion gel filtration chromatography. The purified recombinant *Ov*-M60-like-1 protein was dialysed over phosphate-buffered saline (PBS) and quantified using NanoDrop (ND1000, Thermo Fisher Scientific, USA). The recombinant *Ov*-M60-like-1 protein was stored at -80°C until use.

Mouse anti-*Ov*-M60-like-1 antibody production

Two-week-old BALB/c mice were cared in the animal unit and controlled under the National Experimental Animal Center standard at the Northeast Animal Laboratory Center (NELAC), Khon Kaen University. All protocols were approved by the KKKU Animal Ethics Committee (IACUC KKKU 30/62). Mice were immunized subcutaneously with the purified *Ov*-M60-like-1 protein, 25 μ g in PBS and an equal volume of 2% ammonium hydroxide gel as the adjuvant (Alhydrogel[®], InvivoGen, CA, USA). Two

consecutive boosters of equal dose after 2 weeks were applied on a biweekly basis. The sera-polyclonal antibody of *Ov*-M60-like-1 was collected at 2 weeks after the last booster by intracardiac puncture.

Immunolocalization of *Ov*-M60-like-1 in *O. viverrini* and biliary epithelium

Immunolocalization of *Ov*-M60-like-1 was detected using the streptavidin–biotin immunoperoxidase technique as described previously (Suttiprapa *et al.*, 2009) with a minor modification. The immunohistochemical staining was applied to the 4 μ m paraffin-embedded liver sections of the *Ov*-infected hamsters. The sections were dewaxed and hydrated in the series of xylene, serial ethanol and distilled water. Then, they were placed in 10 mM citrate buffer (pH 6) and the antigen was retrieved under high pressure and temperature for 10 min. Endogenous peroxidase was blocked by treating with methanol–5% H_2O_2 solution for 30 min, and the slides were washed under running tap water and PBS. Non-specific antigens were blocked using 5% normal horse serum for 1 h at room temperature, followed by primary antibody, polyclonal mouse anti-*Ov*-M60-like-1 (at a concentration of 1:50) incubation at room temperature overnight in a moistened chamber. Next, the samples were rinsed with PBS on the shaker for 5 min. This step was repeated thrice. Biotinylated goat anti-mouse immunoglobulin G (1:200, Abcam plc, Cambridge, UK) was applied for 1 h, followed by streptavidin for 30 min (1:300, Zymed, USA). Visualization was performed by 0.05% of 3,3'-diaminobenzidine-tetrahydrochloride (Sigma Aldrich, Germany) and counterstained with Mayer's haematoxylin; then dehydrated, cleared and mounted (Permount, USA). Non-labelled tissues were included as a negative control. *Opisthorchis viverrini* worm was used as a positive control.

Mucinase assay with periodic acid Schiff's-Alcian blue (PAS-AB) staining

Based on the *in vitro* functional activity of *Ov*-M60-like-1 mucinase against bovine sub-maxillary mucin (Ta *et al.*, 2020), the study was raised to evaluate enzyme activity detection on rodent tissues. Three concentrations of recombinant *Ov*-M60-like-1 in 20 mM Tris buffer (pH 6) were applied on the liver tissue sections of *Ov*-infected hamsters and mice at different incubation durations: 40 $\mu\text{g mL}^{-1}$ for 6 h, 4 $\mu\text{g mL}^{-1}$ for 14 h and 1 $\mu\text{g mL}^{-1}$ for 20 h at 37°C. Then, the treated (with *Ov*-M60-like-1) and non-treated (without *Ov*-M60-like-1) slides were washed with 20 mM Tris buffer thrice for 5 min each, followed by mucin histochemistry staining with PAS-AB as previously described (Bancroft *et al.*, 1990). The hamster intestine section was chosen as a positive control.

A combination staining of AB (pH 2.5) with PAS was employed to distinguish acid and neutral mucins (Bancroft *et al.*, 1990). A minor modification was achieved so that hydrated tissue sections were stained with AB (pH 2.5) diluted in 3% acetate buffer (Merck, Germany) for 1 h, then dipped in 3% acetate buffer and washed under running tap water for 5 min; this dipping and washing was repeated for 3 consecutive cycles. Next, the slides were stained in periodic acid (Sigma Aldrich, Germany) for 15 min, and then incubated with Schiff's reagent (Sigma Aldrich, Germany) for 1 h. The nuclei were counterstained with Mayer's haematoxylin (Sigma Aldrich, Germany) for 3 min, then rinsed under running tap water for 5 min, dehydrated, cleared and mounted with Permount (Fisher Scientific, USA).

Preparation of cryosections for mucinase assay

Fresh liver tissue samples of *O. viverrini*-infected hamsters and mice (3 samples of each animal) were trimmed to size 1x1x0.5 cm. Tissues were then rested in the optimal cutting temperature (OCT) compound (Shandon, Cryometrix, Thermo Scientific, UK) at the bottom of metal mold and allowed to freeze at -20°C in freezer. The tissue block was placed in the cutting chamber of cryostat (Microm, HM 525, Thermo Scientific, UK) for 30–60 min to attain an equilibrium temperature. At the appropriate orientation, blocks were cut in $5\ \mu\text{m}$ thickness and then transferred to adhere to the positively charged glass slide (Superfrost Plus, Fisher Scientific, PA, USA) at room temperature. The slides were air-dried for 30–60 min to melt and remove the OCT, and then rinsed in washing buffer. Slides then were incubated with rOv-M60-like-1 ($4\ \mu\text{g mL}^{-1}$) in 20 mM Tris buffer (pH 6) at 37°C for 20 h and washed with tap water before staining (PAS-AB histochemistry).

Data analysis

Colour intensity of peroxidase-immunohistochemical staining was determined for the quantitative analysis of localization and distribution of the Ov-M60-like-1 mucinase. The descriptive interpretation was categorized as strong (+++), moderate (++) and weak (+) colour of immunoreactivity. No colour was described as a negative reaction (Rizzardi *et al.*, 2012; Wattanavises *et al.*, 2019). Blue staining of carbohydrates containing the carboxyl group by AB was determined as acid mucin, while the neutral mucin containing oxidizable vicinal diols was stained magenta with the PAS reagent (Ueda *et al.*, 1994). Mucinase activity was evaluated from the mucin scores based on the colour intensity of PAS-AB staining and the percentage of distribution (Wattanavises *et al.*, 2019) undertaken by 3 competent observers. Mucin staining colour intensity was scored 0 (absence of the colour), 1 (mild or faded colour), 2 (moderately stained) and 3 (strongly stained). The mucin score was statistically analysed using the Mann–Whitney *U* test to compare mucin scores between Ov-M60-like-1 mucinase treated and non-treated groups. A *P* value less than 0.05 illustrates significance.

Results

Immunolocalization of Ov-M60-like-1 in the liver of hamsters

The immunohistochemistry revealed that the Ov-M60-like-1 mucinase is present in both *O. viverrini* tissues and the biliary epithelium of infected hamsters. The staining was widely observed in multiple organs of adult *O. viverrini* with different expression levels. Immunohistochemical features, colour intensity, localization and distribution of Ov-M60-like-1 are shown in Fig. 1 and Table 1. The highest expression in *O. viverrini* worms was observed in the tegumental membrane, tegumental cells, vitelline glands and miracidium within eggs. A moderate expression was diffusely distributed in the gut epithelium, testis and seminal receptacle, but scattered in the ovary. Some parenchymal cells showed weak staining, whereas those in the uterus did not exhibit immunoreactivity. Higher magnification showed strong multifocal expression in rounded dense bodies of the vitelline follicles along with some glands in the miracidium inside of the mature eggs. Ov-M60-like-1 was distinctively expressed among oocytes and also localized in the seminal receptacle.

In the host hamster, the Ov-M60-like-1 was detected in granule-like patterns at the apical cytoplasm of cholangiocytes (Fig. 1B–I). Such granules were observed both in the pre-secreting and post-secreting goblet cells. Occasionally, a strong positive reaction was found scattering on the surface of biliary epithelial

cells, including a mixture of secret substances in the bile duct lumen (Fig. 1B–I and Table 2). Further investigation using PAS-AB staining revealed the co-localization of Ov-M60-like-1 within a mixture of neutral and acid mucins (Fig. 1I). There was no immunoreactivity in the negative control (Fig. 1A). Immunolocalization of Ov-M60-like-1 at the host–parasite interface was identified on the tegument and tegumental cells of *O. viverrini* as well as at the apical compartment of biliary epithelial cells (Fig. 1B–I).

Recombinant Ov-M60-like-1 mucinase assay

The recombinant Ov-M60-like-1 mucinase activity against the worm and the bile duct of Ov-infected hamster together with the identification of the mucin types of worms and the host using PAS-AB histochemistry were described. Mucin digestion activity assay was employed at different incubation times and enzyme concentrations to find out the maximum activity. Mucinase activity was apparently detected in the samples being treated with $40\ \mu\text{g mL}^{-1}$ (1 dose) of mucinase for 14 h; $4\ \mu\text{g mL}^{-1}$ (1/10 dose) for 14 and 20 h; however, there was no sign of digestion in the samples with $40\ \mu\text{g mL}^{-1}$ mucinase treatment for 6 h and the negative control slide (Fig. 2). Histologically, rOv-M60-like-1 was capable of digesting neutral mucin in the parenchyma, seminal receptacle and testis of the worm (Table 3). It can also digest neutral mucin in the goblet cells of the host bile duct. There was no digestion of mucin in the tegument, tegumental cells and vitelline glands of the worm. Losing of PAS magenta colour after rOv-M60-like-1 treatment indicated the effect on the neutral mucin. In addition, the mixture type of mucin (purple) lost the neutral mucin (magenta) after digestion with $4\text{--}40\ \mu\text{g mL}^{-1}$ at 14–20 h resulting in the change of colour from purple to blue. Alternatively, the acid mucin (blue) located in the uterus and gut epithelia of *O. viverrini* have not been affected.

Mucinase activity of Ov-M60-like-1 was able to modify the native globule structure of mucin in the goblet cells to be expanded and spread out (Figs 2 and 3), as compared to the non-treated control group where the mucin is intact in the goblet cells. Results from PAS-AB histochemical staining showed the presence of mixture mucin in the goblet cells and the mucus among cholangiocytes of the *O. viverrini*-infected hamsters (Table 4). In contrast, rOv-M60-like-1 mucinase could not digest the acid and neutral mucin/mucus as well as the mixture of both mucin types in the bile duct of *O. viverrini*-infected mice (Table 4). The structure of mucin in the goblet cells and in the lumen of the bile duct of mice was still intact even being incubated with rOv-M60-like-1 mucinase for 20 h, despite the fact that mucins in the cholangiocyte were also digested (Fig. 3). The analysis of mucin scores showed that the Ov-M60-like-1 treated group was significantly reduced in hamster's tissue ($P < 0.01$ from Mann–Whitney *U* test); however, there was no significant difference between the treated and untreated groups of mice ($P = 0.074$) (Table 5).

Given that this research aimed to study the localization of the mucinase enzyme and its function in the tissue where the worm is dwelling, the enzyme's location and its substrate in the tissue need to be precisely identified. The frozen sections have several limitations especially cytological and architectural distortion and artefacts. Therefore, we chose to perform the functional analysis in the paraffin section to give a clear illustration of tissue structures. Nevertheless, to confirm that the distinction of mucinase activity was not due to the effect of formalin or paraffin during tissue fixation and processing, we performed another mucinase assay on the frozen tissue. Unsurprisingly, the result was similar to the paraffin section. The mucinase from *O. viverrini* could digest the

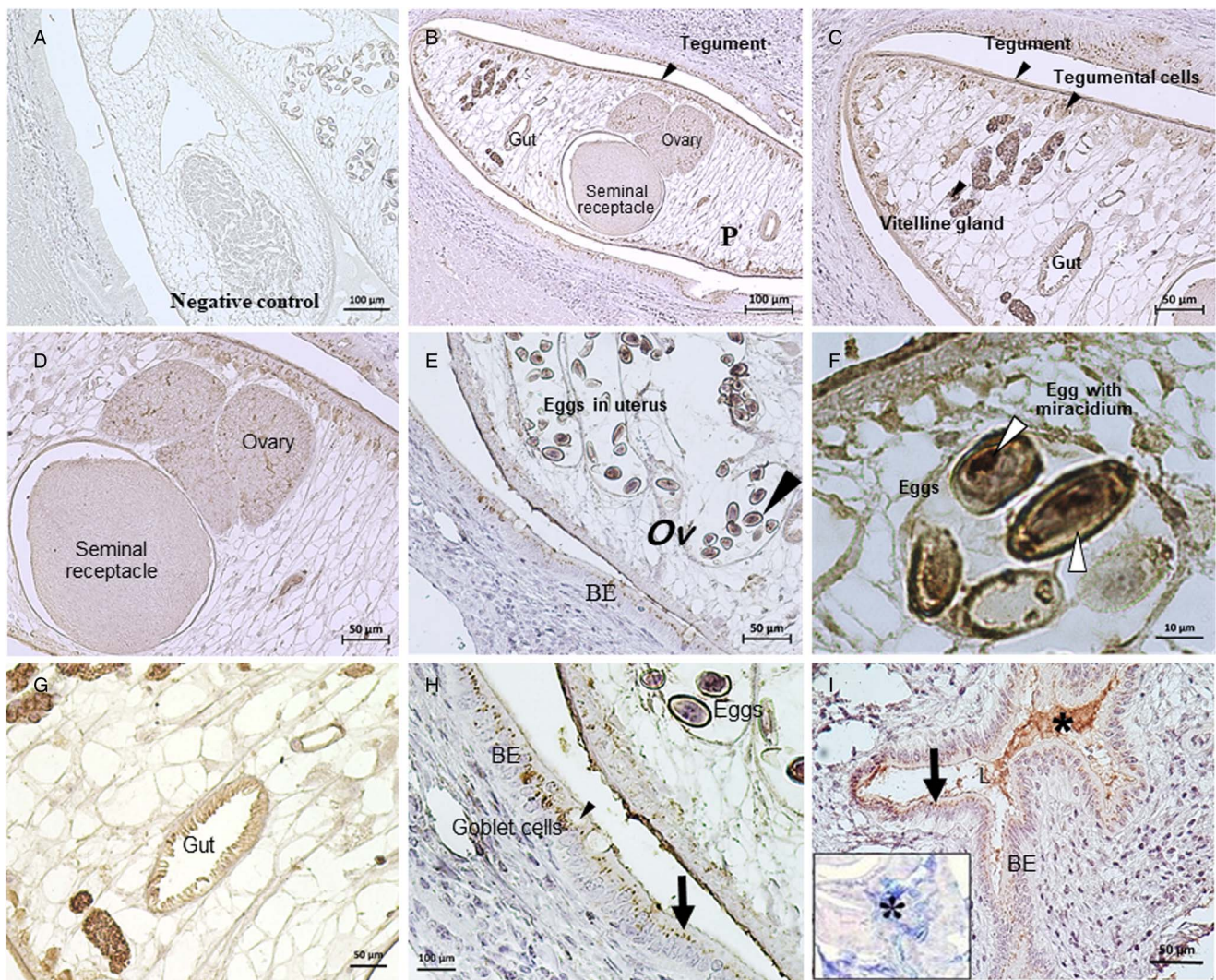


Fig. 1. Immunolocalization of *Ov*-M60-like-1 in *Opisthorchis viverrini* (*Ov*) and the bile duct of hamsters at day 56 p.i. Negative control of adult *O. viverrini* and the biliary epithelium (BE) was shown in (A). (B–I) represent positive expression of *Ov*-M60-like-1 both in BE and various organs of *O. viverrini*, i.e. gut, tegument, tegumental cells, vitelline glands, testis, ovary and embryonated eggs with miracidia in the uterus (white arrowheads). Positive immunostaining was also found in granules in either intact or secreting goblet cells and at the apical compartment of BE (black arrows, H–I). *Ov*-M60-like-1 mucinase in the lumen of bile duct co-localized with host mucus being examined with PAS-AB staining (*, I inset).

Table 1. Immunoreactivity of *Ov*-M60-like-1 in the adult *Ov* residing in the bile duct of hamsters at day 56 p.i.

Structure	Intensity	Distribution	Description
Tegument	+++	Diffuse	Homogenous strong stain diffusely distributed at the syncytial tegument including its basal and outer membrane.
Tegumental cells	+++	Diffuse	Non-homogenous strong (mostly in tegumental granules) and moderate staining (in cytoplasm and cell processes) diffusely distributed among the isolated and group of cells.
Parenchyma	+	Diffuse	Homogenous weak stain diffusely distributed among matrices.
Ovary	++	Scattered	Homogenous moderate stain scattered in the oocytes.
Vitelline glands	+++	Diffuse	Homogenous strong stain multifocally distributed in vitelline follicles, particularly at the peripheral cytoplasm with dense nuclei of stem or undifferentiated vitelline cells.
Eggs	+++	Scattered	Non-homogenous strong (particularly in cephalic and secretory glands of miracidia) and moderate stain multifocally distributed in the embryonated eggs.
Uterus	–	Diffuse	Homogenous moderate stain diffusely distributed in the sperm.
Testis	++	Diffuse	Homogenous moderate stain diffusely distributed in the sperm.
Gut epithelia	++	Diffuse	Homogenous moderate stain diffusely distributed in gastrodermal villi and crypt.
Oral sucker	nd	nd	nd
Ventral sucker	nd	nd	nd

+++ , strong; ++ , moderate; + , weak; – , negative; nd , not determined.

Table 2. Immunoreactivity of *Ov*-M60-like-1 in the bile duct of hamsters at day 56 p.i.

Structure	Intensity	Distribution	Description
Cilia	++	Scattered	Homogenous moderate stain on surface of biliary epithelial cells.
Goblet cells	+++ +++	Diffuse	Homogenous strong stain of pre-secreting and post-secreting granules in goblet cells.
Apical cytoplasm	+++	Diffuse	Homogenous strong stain of granules in apical cytoplasm of biliary epithelial cells.
Basolateral cytoplasm	–	None	No stain appears.
Nucleus	–	None	No stain appears.
Lumen	+++	Diffuse	Homogenous strong stain of a mixture of <i>Ov</i> -M60-like-1 mucinase and host mucus (with PAS-AB staining) co-localizing in the lumen of the bile duct.

+++; strong; ++, moderate; +, weak; –, negative.

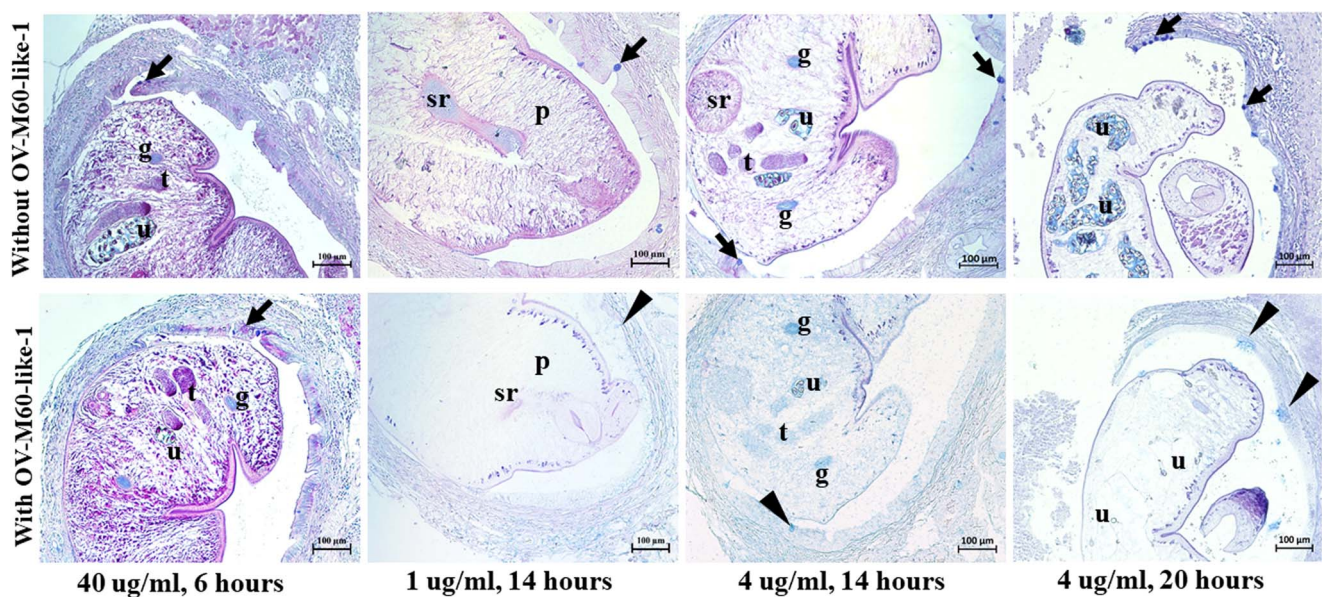


Fig. 2. rOv-M60-like-1 mucinase assay on the infecting *O. viverrini* and the bile duct of *O. viverrini*-infected hamsters, followed by PAS-AB staining for mucin. rOv-M60-like-1 mucinase treatment at $40 \mu\text{g mL}^{-1}$ for 14 h (F), $4 \mu\text{g mL}^{-1}$ for 14 h (G) and $4 \mu\text{g mL}^{-1}$ for 20 h (H) was capable of digesting neutral mucin in the par-enchyma (p), seminal receptacle (sr) and testis (t) of the worm, including mucin in the host goblet cells. No activity was seen in the samples treated with $40 \mu\text{g mL}^{-1}$ of *Ov*-M60-like-1 mucinase for 6 h (E) and those without mucinase treatment (A–D). With PAS-AB staining, the intact mixture of neutral and acidic mucins in (A–E) appeared in purple colour (black arrows). Since the mucinase could digest only neutral mucin, the remaining acidic mucins in the gut epithelium (g), testis (t) and uterus (u) of *O. viverrini* were stained in blue colour (black arrowheads, F–H).

mucin of the hamsters, while there was no digestion of mice tissue (Supplementary Fig. 1); however, the tissue architecture was poorly identified. Therefore, we believe that we chose the proper technique for this research and the results are valid.

Discussion

Recently, the recombinant protein of M60-like-1 (rOv-M60-like-1) metallopeptidase from the excretory–secretory products of *O. viverrini* has been identified and produced (Ta et al., 2020). It was able to digest bovine submaxillary mucin *in vitro*, suggesting its role in mucin degradation. To further characterize this mucinase, here, the immunolocalization and functional assay were performed. The immunohistochemistry revealed that the mucinase is expressed mainly on the tegument, gut and reproductive organs of the mature adult *O. viverrini* worm. In addition, it was also detected on adjacent host biliary cells. The rOv-M60-like-1 mucinase assay demonstrated that the mucinase can digest neutral mucin and modify the structure of the mixture mucin. However, it was unable to digest the acidic mucin of the worm and only

partially digested the acidic mucin in the hamster tissue. In contrast, the acid and neutral mucins as well as the mixture of both mucin types in the bile duct lumen and goblet cells of *O. viverrini*-infected mice were still intact.

Detection of *Ov*-M60-like-1 mucinase in the reproductive organs of the worm, such as testis, ovary, vitelline glands and seminal receptacle reflect its possible roles in egg and sperm development. Its detection in the gut epithelia and the tegument of *O. viverrini* implied this enzyme was released from such structures of the worm, convincing that the mucinase is the major component of OVES (Ta et al., 2020). The distribution of *Ov*-M60-like-1 in the bile duct tissue of hamsters, particularly inside the goblet cells, suggested its role in mucin degradation which is able to breakdown the mucin barrier and facilitate the colonization of the worm in the bile duct.

Localization of *Ov*-M60-like-1 in the bile duct epithelium also implies its role in host–parasite crosstalk. The immunoreactivity pattern among the apical cytoplasm of cholangiocytes in the granular form indicates this mucinase is packaged inside the vesicles. Such findings might be explained similarly to that of the

Table 3. Effects of doses and duration of *Ov*-M60-like-1 treatment on the mucin structures of *Ov* residing in the bile duct of *Ov*-infected hamsters

Structures	M60-like-1 treatment					
	1×, 14 h	Distribution	1/10×, 14 h	Distribution	1/10×, 20 h	Distribution
Tegument	–	–	–	–	–	–
Tegumental cells	–	–	–	–	–	–
Parenchyma	+, N	Diffuse	+, N	Diffuse	+, N	Diffuse
Vitelline glands	–	–	–	–	–	–
Uterus	–	–	–	–	+	Diffuse
Eggs	–	–	–	–	–	–
Testis/ovary	+, M	Diffuse	+, M	Diffuse	+, M	Diffuse
Seminal receptacle	+, M	Diffuse	+, M	Diffuse	nd	–
Gut	–	–	–	–	–	–
Oral sucker	–	–	–	–	–	–
Ventral sucker	–	–	–	–	–	–

+, Digested; –, not digested; nd, not determined; M, mixed mucin; N, neutral mucin; 1×, 40 $\mu\text{g mL}^{-1}$; 1/10×, 4 $\mu\text{g mL}^{-1}$.

Mucinase at any concentration and duration could not alter the mucin of the tegument, tegumental cells, vitelline glands, gut, oral sucker and ventral sucker of the worm. Different modes of digestion were confined on their parenchyma and reproductive organs.

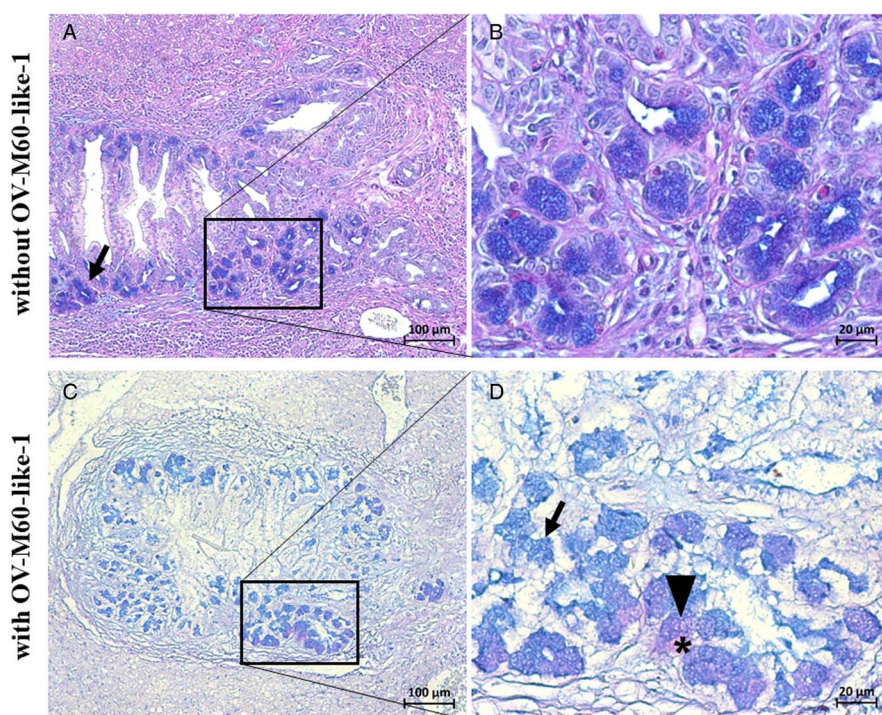


Fig. 3. *rOv*-M60-like-1 mucinase assay in the bile duct of *O. viverrini*-infected mice, followed by PAS-AB staining. Rectangle in (A) was enlarged in (B) and that in (C) was enlarged in (D). The structures with intact mucin mixture either with 4 $\mu\text{g mL}^{-1}$ of *Ov*-M60-like-1 mucinase treatment for 20 h and without treatment were stained in purple colour (arrowheads, B, D). The blue stain (black arrow, D) indicates the main remaining acidic mucin which could not be digested by the mucinase.

secreted extracellular vesicles (EVs) of *Fasciola hepatica*. The antigenic proteins and glycans on the surface of *F. hepatica* EVs contribute to ligand–receptor interactions, initiating vesicle docking, and subsequently being internalized by host epithelial cells (de la Torre-Escudero *et al.*, 2019). The cathepsin L-like protease was found in the vesicles (Dalton *et al.*, 2003). Thus, the *Ov*-M60-like-1 may be transferred to the host *via* vesicles in a similar manner as do in *F. hepatica*. These vesicles are released into the extracellular environment and internalized into the host bile duct epithelial cells by endocytosis similar to the co-culture study of the human cholangiocytes cell line H69 with OVES (Chaiyadet *et al.*, 2015).

The mucinase could partially digest mucins produced by hamsters; however, it could not digest all mucin types (neutral, acidic and mixture) of murine mucins. This *Ov*-M60-like-1 mucinase

may be addressed as mucin-selective protease. Species-specific mucin components are the consequence of host–parasite interaction. Glycan chains of host mucin may be the significant structure for the selective target of certain helminthic mucinase. Thus, host mucin types might serve as a determinant for mucinase (Noach *et al.*, 2017). A well-known representation of excretory/secretory products, a serine protease of *Trichuris muris* can chop the sticky human intestinal mucin/mucus to become depolymerized (Hasnain *et al.*, 2012). Disruption of the intestinal mucus barrier allowed the worm to access epithelial cells of the host. Conversely, mucin alteration in the mice model remains undigested with such enzyme. Differences in mucin digestion among hosts might determine worm expulsion and host susceptibility.

The role of this mucinase in the pathogenesis of *O. viverrini* remains unknown. A previous study demonstrated the OVES

Table 4. Effects of doses and durations of rOv-M60-like-1 treatment on the mucin structures of the biliary epithelium of Ov-infected hamsters and mice

Biliary epithelium	M60-like-1 treatment					
	1×, 14 h	Distribution	1/10×, 14 h	Distribution	1/10×, 20 h	Distribution
Hamsters						
Goblet cell	+, M	Scattered	+, N	Scattered	+, M	Diffuse
Cytoplasm of cholangiocytes	+	Diffuse	–		+	Diffuse
Nucleus of cholangiocytes	+	Diffuse	–		+	Diffuse
Mice						
Goblet cells	–		–		–	
Cytoplasm of cholangiocytes	+	Diffuse	–		+	Diffuse
Nucleus of cholangiocytes	+	Diffuse	–		+	Diffuse

+, digested; –, not digested; M, mixed mucin; N, neutral mucin.

Mucinase at any concentration and duration could not digest mucin in the goblet cells of mice. Negative results were found in hamsters (except in goblet cells) and mice with 1/10 dose of mucinase treatment for 14 h.

Table 5. Statistical analysis results of Ov-M60-like-1 mucinase activity

Group	Mucin scores		P
	Treated median (min–max)	Non-treated median (min–max)	
Hamsters (n = 9)	0 (0–1)	3 (3–3)	<0.01**
Mice (n = 18)	3 (3–3)	3 (3–3)	0.074

**P < 0.01 from the Mann-Whitney U test.

induces Toll-like receptor 4 upregulation and production of interleukin 6 (IL-6) and IL-8 in human cholangiocytes (Ninlawan et al., 2010). The M60-like metalloprotease YghJ from *E. coli* stimulated the secretion of cytokines IL-1 α , IL-1 β and tumour necrosis factor- α in murine macrophages (RAW 264.7) and IL-8 from human intestinal epithelial cells (HT-29) through Toll-like receptor 2-dependent macrophage activation and nuclear factor- κ B and mitogen-activated protein kinase signalling pathway (Tapader et al., 2018). In a similar fashion, Ov-M60-like-1, which is the major component of OVES, might induce a pro-inflammatory response. This hypothesis warrants further investigation.

In conclusion, strong immunoreactivity and diffuse distribution of the Ov-M60-like-1 was detected at the fluke tegument and tegumental cells as well as in the apical cholangiocytes and the goblet cells of the host. These suggest a possible role of Ov-M60-like-1 mucinase in the host–parasite interaction. Additionally, expression in multiple organs of the worm indicates the housekeeping task of this enzyme. Also, the rOv-M60-like-1 mucinase assay revealed significant roles of this enzyme in *O. viverrini* parasitism which altered the host mucus barrier by digestion of both acidic and neutral mucins. All types of mucin produced by the non-susceptible host may be a protective barrier against such mucinase. Further functional profiles of the Ov-M60-like-1 mucinase and its inhibitors may highlight its crucial roles in host–parasite interaction and targets for diagnostics and therapeutic candidates.

Supplementary material. The supplementary material for this article can be found at <https://doi.org/10.1017/S0031182022000403>.

Acknowledgements. The authors thank Professor Yukifumi Nawa for reviewing and revising this manuscript. The authors also thank Professor

Banchob Sripa for supervising this study. The authors express their gratitude to Miss Jiraporn Jumpajan for her assistance with recombinant protein production. W. D. W. received the KKKU Active Recruitment Scholarship (2018) for her doctoral study.

Author contributions. S. T., P. S., P. T. and S. S. conceived and designed the study. W. D. W., B. T. T. T. and A. R. K. C. conducted experiments. All authors contributed to data analysis. W. D. W., S. T., P. S., P. T. and S. S. wrote the first draft of the manuscript. ST and SS edited and finalized the manuscript.

Financial support. The study was partly funded by Khon Kaen University and the Faculty of Veterinary Medicine (KKU Vet. Res. VM007/2564).

Conflict of interest. The authors declare there are no conflicts of interest.

References

- Bancroft J, Stevens A and Toner D (1990) *Theory and Practice of Histological Techniques*, 3rd Edn. Edinburgh, UK: Churchill Livingstone Elsevier.
- Chaiyadet S, Smout M, Johnson M, Whitchurch C, Turnbull L, Kaewkes S, Sotillo J, Loukas A and Sripa B (2015) Excretory/secretory products of the carcinogenic liver fluke are endocytosed by human cholangiocytes and drive cell proliferation and IL6 production. *International Journal for Parasitology* **45**, 773–781.
- Dalton JP, Neill SO, Stack C, Collins P, Walshe A, Sekiya M, Doyle S, Mulcahy G, Hoyle D, Khaznadj E, Moiré N, Brennan G, Mousley A, Kreshchenko N, Maule AG and Donnelly SM (2003) *Fasciola hepatica* cathepsin L-like proteases: biology, function, and potential in the development of first generation liver fluke vaccines. *International Journal for Parasitology* **33**, 1173–1181.
- de la Torre-Escudero E, Gerlach JQ, Bennett APS, Cwiklinski K, Jewhurst HL, Huson KM, Joshi L, Kilcoyne M, O'Neill S, Dalton JP and Robinson MW (2019) Surface molecules of extracellular vesicles secreted by the helminth pathogen *Fasciola hepatica* direct their internalisation by host cells. *PLoS Neglected Tropical Diseases* **13**, e0007087.
- Hasnain SZ, McGuckin MA, Grecnis RK and Thornton DJ (2012) Serine protease(s) secreted by the nematode *Trichuris muris* degrade the mucus barrier. *PLoS Neglected Tropical Diseases* **6**.
- Hasnain SZ, Gallagher AL, Grecnis RK and Thornton DJ (2013) A new role for mucins in immunity: insights from gastrointestinal nematode infection. *International Journal of Biochemistry & Cell Biology* **45**, 364–374.
- He C and Ohnishi K (2017) Efficient renaturation of inclusion body proteins denatured by SDS. *Biochemical and Biophysical Research Communications* **490**, 1250–1253.
- Linden S, Sutton P, Karlsson N, Korolik V and McGuckin M (2008) Mucins in the mucosal barrier to infection. *Mucosal Immunology* **1**, 183–197.
- Lvova MN, Tangkawattana S, Balthaisong S, Katokhin AV, Mordvinov VA and Sripa B (2012) Comparative histopathology of *Opisthorchis felineus* and *Opisthorchis viverrini* in a hamster model: an implication of high pathogenicity of the European liver fluke. *Parasitology International* **61**, 167–172.

- Ninlawan K, O'Hara SP, Splinter PL, Yongvanit P, Kaewkes S, Surapaitoon A, LaRusso NF and Sripa B (2010) *Opisthorchis viverrini* excretory/secretory products induce Toll-like receptor 4 upregulation and production of interleukin 6 and 8 in cholangiocyte. *Parasitology International* **59**, 616–621.
- Noach I, Ficko-Blean E, Pluvinage B, Stuart C, Jenkins ML, Brochu D, Buenbrazo N, Wakarchuk W, Burke JE and Gilbert M (2017) Recognition of protein-linked glycans as a determinant of peptidase activity. *Proceedings of the National Academy of Sciences of the USA* **114**, E679–E688.
- Rizzardi AE, Johnson AT, Vogel RI, Pambuccian SE, Henriksen J, Skubitz AP, Metzger GJ and Schmechel SC (2012) Quantitative comparison of immunohistochemical staining measured by digital image analysis versus pathologist visual scoring. *Diagnostic Pathology* **7**, 1–10.
- Suttiaprapa S, Mulvenna J, Huong NT, Pearson MS, Brindley PJ, Laha T, Wongkham S, Kaewkes S, Sripa B and Loukas A (2009) Ov-APR-1, an aspartic protease from the carcinogenic liver fluke, *Opisthorchis viverrini*: functional expression, immunolocalization and subsite specificity. *International Journal of Biochemistry & Cell Biology* **41**, 1148–1156.
- Suttiaprapa S, Sotillo J, Smout M, Suyapoh W, Chaiyadet S, Tripathi T, Laha T and Loukas A (2018) *Opisthorchis viverrini* proteome and host–parasite interactions. *Advances in Parasitology* **102**, 45–72.
- Ta BT, Nguyen DL, Jala I, Dontumpri R, Plumworasawat S, Aighewi O, Ong E, Shawley A, Potriquet J, Saichua P, van Diepen A, Sripa B, Hokke CH and Suttiaprapa S (2020) Identification, recombinant protein production, and functional analysis of a M60-like metallopeptidase, secreted by the liver fluke *Opisthorchis viverrini*. *Parasitology International* **75**, 102050.
- Tapader R, Bose D, Dutta P, Das S and Pal A (2018) SsLE (YghJ), a cell-associated and secreted lipoprotein of neonatal septicemic *Escherichia coli*, induces Toll-like receptor 2-dependent macrophage activation and proinflammation through NF- κ B and MAP kinase signaling. *Infection and Immunity* **86**, e00399-18.
- Theodoropoulos G, Hicks SJ, Corfield AP, Miller BG and Carrington SD (2001) The role of mucins in host–parasite interactions: part II – helminth parasites. *Trends in Parasitology* **17**, 130–135.
- Ueda T, Mittal AK, Fujimori O and Yamada K (1994) HID-AB2.5-PAS and HID-PAS methods for the histochemical analyses of a variety of carbohydrates. *Okajimas Folia Anatomica Japonica* **71**, 51–57.
- Wattanavises S, Silsirivanit A, Sawanyawisuth K, Cha'on U, Waraasawapati S, Saentaweesuk W, Luang S, Chalermwat C, Wongkham C and Wongkham S (2019) Increase of MAL-II binding alpha2,3-sialylated glycan is associated with 5-FU resistance and short survival of cholangiocarcinoma patients. *Medicina (Kaunas)* **55**, 761.